THE ASTROPHYSICAL JOURNAL, **191**: 143–155, 1974 July 1

Fe I FLUORESCENCE IN T TAURI STARS

L. A. WILLSON*
Department of Astronomy, University of Michigan, Ann Arbor
Received 1973 November 14

ABSTRACT

A statistical equilibrium analysis for the selective excitation of λλ4063, 4132 of Fe I shows: (*a*) selective excitation by Ca II or Hϵ can reproduce the line intensities observed in T Tauri stars; (*b*) when enhanced λλ4063, 4132 emission is observed, an upper limit on the electron density and/or hydrogen density as a function of distance from the star is obtained; (*c*) it is sometimes also possible to obtain an upper limit on the local gas kinetic temperature and a lower limit on the hydrogen density divided by the dilution factor W. Upper limits obtained for RW Aurigae are: $N_e/W \leq 10^{16}$ and $N_H/W \leq 10^{16}$ if H II/H I ≤ 0.1, for $T_e = 3000°$ K. Also, $N_H/W > 10^{14}$ if the lines are formed less than 1000 stellar radii from the star. A qualitative model is suggested for RW Aurigae where the Fe I lines are formed in an expanding envelope, beyond 10 stellar radii from the central star. Although Ca II H is a stronger emission line than Hϵ in some T Tauri stars, considerations of the velocity shifts expected for different parts of the envelope indicate that Hϵ may be responsible for the selective excitation of λλ4063, 4132.

Subject headings: atomic processes — emission-line stars — pre-main-sequence stars

I. INTRODUCTION

The Fe I emission lines λλ4063, 4132 are enhanced in T Tauri stars relative to the other lines of the same multiplet (see e.g., Joy 1945). This may be explained in terms of a fluorescent mechanism due to the wavelength coincidence of the strong Ca II H and Hϵ emission around λ3969 with the transition $a\,^3F_4$–$y\,^3F_3^o$ of Fe I λ3969.261 (Herbig 1945). We expect that under conditions of sufficiently low electron density and temperature the level $y\,^3F_3^o$ will be strongly overpopulated, leading to emission in lines originating from it (see fig. 1).

This paper presents a statistical equilibrium analysis of this set of lines, with three goals. The first is to see if reasonable assumptions for the physical conditions will lead to the observed line ratios. This is simply a quantitative examination of the fluorescent mechanism. The second is to determine the effect of several parameters on the line ratios observed. Finally, we would like to determine the range of conditions for which enhanced λλ4063, 4132 emission is possible. This will enable us to use the observed line ratios to obtain limits on the physical conditions.

II. THE MODEL AND ASSUMPTIONS

a) *The Mechanism and the Model Atom*

A 12-level model Fe I atom with continuum is shown in figure 1. Calculations were also made with a five-level model atom: levels 1, 2, 3, 10, and 11 on the figure. This five-level atom contains the essential physics of the mechanism. Level 1 is the lower level of the pumped transition λ3969. Levels 2 and 3 are the lower levels of the observable lines λλ4063, 4132, and 4143. The lines λλ4063 and 4132 originate from the pumped level 11. Level 10 is not pumped and the line λ4143 which comes from it is thus a suitable "comparison" line.

A comparison of the results of the five-level and 12-level calculations shows that the five levels do indeed contain the essential physics of the mechanism. Calculations were also made with a 12-level atom containing the ground state of Fe I, $a\,^5D_{1,2,3,4}$, instead of the levels $a\,^3G_{4,5}$ and $b\,^3G_{4,5}$. A comparison of representative curves obtained from these three model atoms showed that the differences are not large enough to significantly affect our conclusions—the maximum difference was 0.1 in the log, and all features of the curves were the same.

Since the principal transitions we are concerned with, those of the five-level model atom, are within a single multiplet, uncertainties in the iron *f*-values should have little effect on our results. In fact, computations made with *gf*-values differing by a factor of 3 gave identical results.

Two line ratios will be considered: λ4063/λ4143 for the five-level atom, and in addition λ4063/λ4005 for the 12-level atoms. The ratio λ4063/λ4143 indicates the relative populations of levels 10 and 11; λ4063/λ4005 indicates the relative populations of levels 11 and 12. These two line ratios thus represent two possible configurations: (1) a comparison line originating from a level below the overpopulated level and (2) a comparison line originating from a level above the overpopulated level. The results show that these two line ratios can behave quite differently (see § III*a*).

b) *The Fine-Structure Transitions*

Preliminary calculations showed that collisional transitions between fine-structure levels are important in determining when enhanced λλ4063, 4132 emission will occur. As was pointed out by Bahcall and Wolf (1968) collisions with protons and with neutral atoms are more important for fine-structure transitions in neutral atoms than are electronic collisions.

* Present address: Erwin W. Fick Observatory, Department of Physics, Iowa State University, Ames, Iowa 50010.

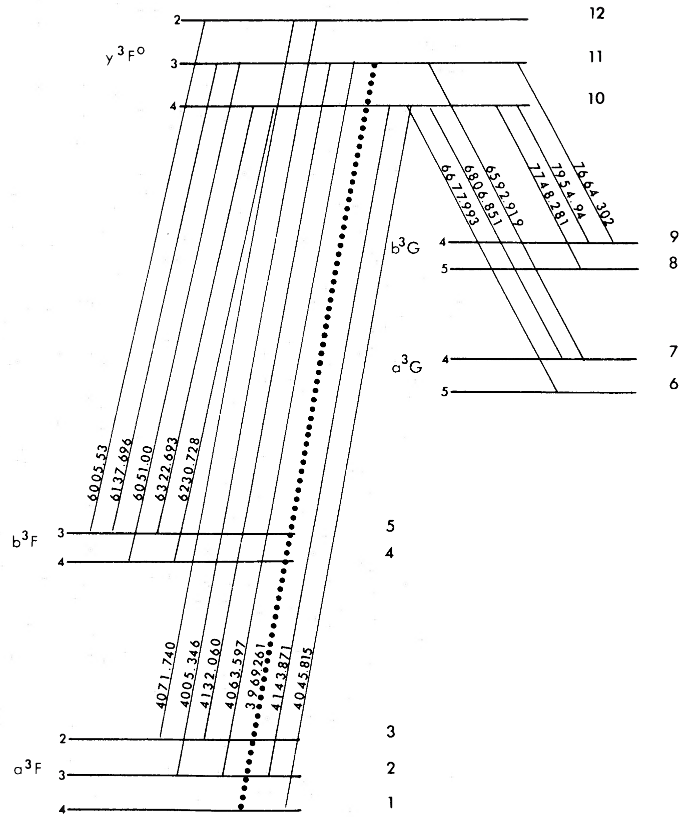

FIG. 1.—The model atom. The numbers 1–12 on the right refer to the 12-level model atom. The five-level model consists of levels 1, 2, 3, 10, and 11 of the 12-level atom. The dotted line is the pumped transition λ3969.

The relevant averaged cross-sections times velocity for neutral iron are (i) for electronic collisions:

$$\langle \sigma v \rangle_e \lesssim 10^{-10} \quad \text{for } T \lesssim 10^5 \text{ °K}, \tag{1}$$

estimated from the calculations of Breig and Lin (1966) for neutral oxygen; (ii) for collisions with protons:

$$\langle \sigma v \rangle_p \simeq \begin{cases} 10^{-14} T^{3/2} P(i \to f) \left(\dfrac{0.7}{\Delta E} \right)^2 & \text{if } T \leq 10^4 \text{ °K}, \\ 2.5 \times 10^{-8} P(i \to f) & \text{if } T \geq 10^5 \text{ °K}, \end{cases} \tag{2}$$

from Bahcall and Wolf (1968).

These relations should be valid to within a factor of 2, with $P(i \to f)$ given by Bahcall and Wolf (1968, eqs. [48]–[52]); and (iii) for collisions with neutral hydrogen atoms:

$$\langle \sigma v \rangle_{\rm H} \simeq 2 \times 10^{-9} (T/100)^{1/6} P(i \to f), \tag{3}$$

again from Bahcall and Wolf. The factor $P(i \to f)$ is the probability the ion goes from the state i to the state f after a strong collision. The assumption that after a strong collision the states will be populated according to their degeneracies gives

$$P(i \to f) \simeq g_f \Big/ \sum_j g_j . \tag{4}$$

Bahcall and Wolf also give equations for $P(i \to f)$ for the low-temperature ($T \leq 10^3$ °K) limit, where equation (4) no longer holds.

For neutral iron for the transition between our levels (2) and (1) we find $\langle \sigma v \rangle_{\rm H} \geq \langle \sigma v \rangle_p$ in the temperature range of interest, so that unless the hydrogen is mostly ionized we need only worry about collisions with neutral hydrogen atoms. This is very fortunate, since it means that we do not have to know the details of the ionization equilibrium as long as H II/H I $\lesssim 0.1$. For RW Aur this must certainly be the case, because the fluorescent iron lines must be formed in a region with *neutral* iron.

Figure 2 shows the results of calculations done with $N_e/N_{\rm H}$ ranging from 1 to 10^{-4}. For $N_e/N_{\rm H} \simeq 1$ electron collisional excitation of permitted transitions determine the high-density section of the curve, but for $N_e/N_{\rm H} \ll 1$ fine-structure transitions by collision with neutral hydrogen atoms are dominant at all densities.

The remainder of the calculations of this paper were done with $N_e/N_{\rm H} = 0.01$, corresponding to the hydrogen being 1 percent ionized. The conclusions resulting are valid for hydrogen between 0 and 10 percent ionized. Both collisions with protons and collisions with neutral hydrogen were included in the calculations, although proton collisions had no significant effect on the results.

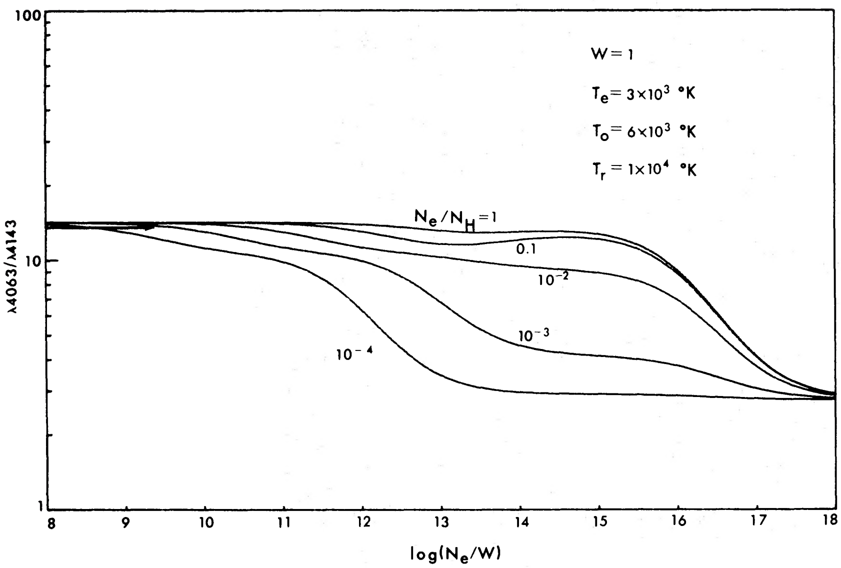

FIG. 2*a*

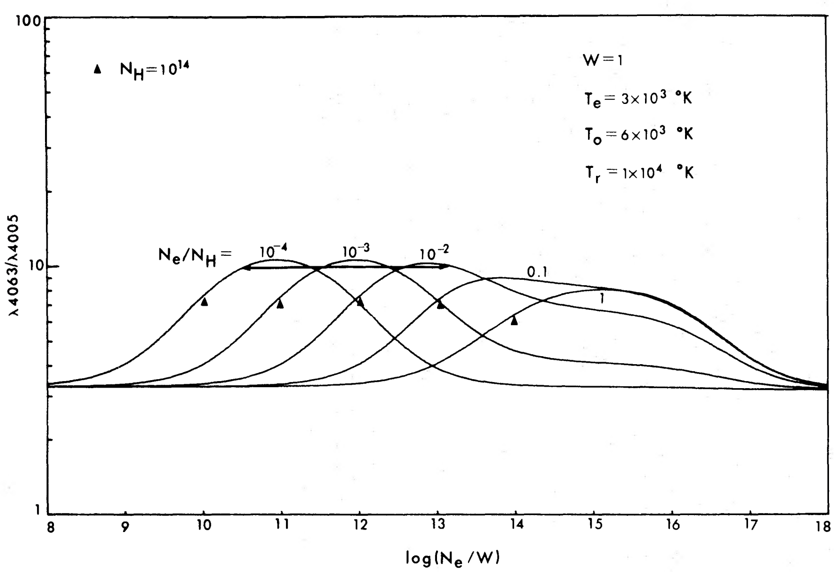

FIG. 2*b*

FIG. 2.—(*a*) and (*b*). Results for different ionization equilibria, represented by different values of N_e/N_H. The observed values of the line ratios, from Gahm (1970), are shown by horizontal arrows. $N_H = 10^{14}$ is marked for each curve; this is the lower limit on N_H for all N_e/N_H shown.

c) The Model

Details of the radiative transfer in the lines have not been included in this preliminary analysis. The lines λλ4063 and 4132 both originate from the pumped level 11; if the lines are optically thin, the ratio of intensities of these two lines must be approximately equal to the ratio of their *A*-values, 3.7. (For a discussion of this test, see Willson 1972). But for the three plates of RW Aur measured by Gahm (1970) these ratios are between 1.4 and 1.8. Thus it may not be reasonable to suppose that for RW Aur these lines are optically thin. We can estimate the effect of increased optical depth in these lines on our results by a simple argument. Define $\mathscr{N}$ by assuming that the radiative de-excitation rate is $\mathscr{N}$ times the collisional rate, i.e.,

$$\sum_i R_{11,i} = \mathscr{N} \sum_i C_{11,i} \,. \tag{5}$$

Then for every $\mathscr{N}$ absorptions of a photon in one of the fluorescent lines there will be a collisional transition instead of reemission of another enhanced line. This will drive the line intensities toward their LTE values. Under typical conditions $\mathcal{N}$ is about 10. As the density or temperature increases, collisions become more important, and $\mathcal{N}$ decreases. As is discussed in detail § III, the statistical equilibrium calculations given an upper limit on the densities for which enhanced λλ4063, 4132 emission is expected. The effect of increased optical depth on our results is therefore to *decrease* the upper limit on the electron density.

Conditions in the vicinity of the Fe I atom may be characterized by five parameters. Collisional transition rates require knowledge of N_e and T_e, the electron temperature and density at the position of the iron atom. The background radiation field is described by T_0, a blackbody temperature giving the continuum energy distribution. T_r is a similar parameter specifying the intensity of the exciting λ3969 line. W is a dilution factor, primarily geometric, which is always ≤ 1. We assume that the same dilution factor applies to the continuum and to the Ca II H-line; this is true for example if W is purely geometric and if the Ca II emission originates close to the star. T_r may be adjusted to compensate for small differences in W. For

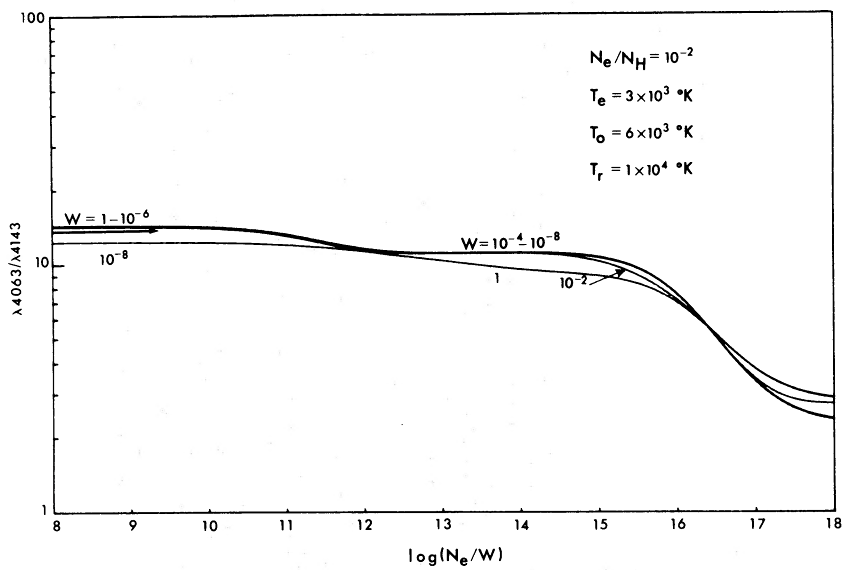

FIG. 3*a*

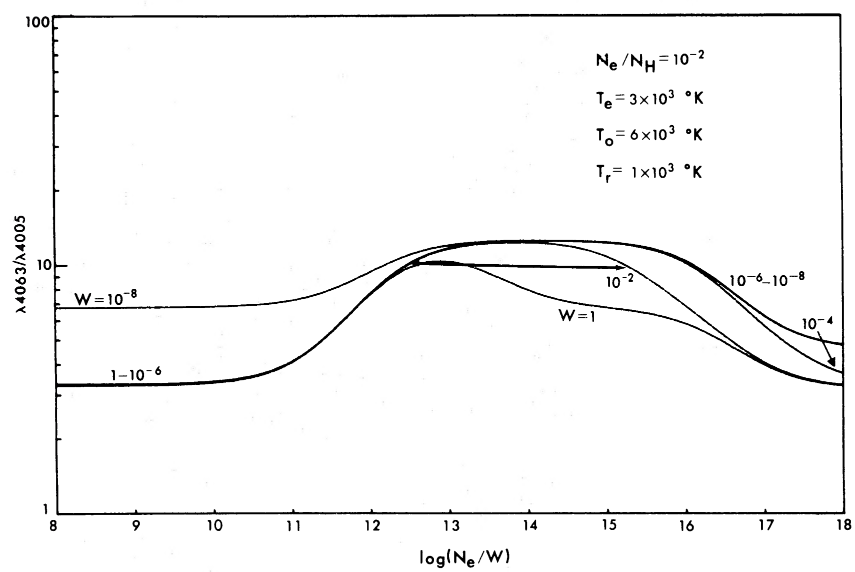

FIG. 3*b*

FIG. 3.—(*a*) and (*b*). The ratios λ4063/λ4143 and λ4063/λ4005 as a function of log (N_e/W) for values of W between 1 and 10^{-12}. For $W \geq 10^{-6}$, all the important features of the curves remain unchanged as W varies. The line ratios observed in RW Aur are indicated by arrows as in fig. 2.

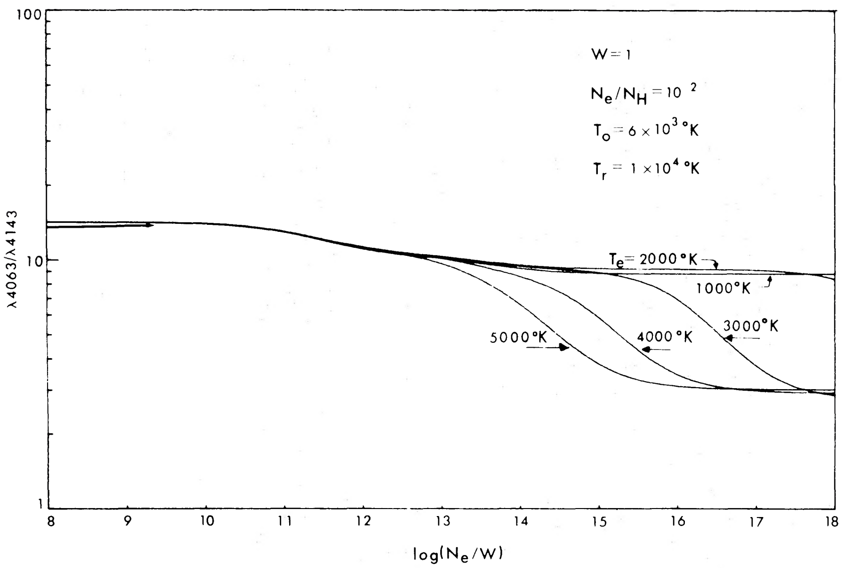

FIG. 4a

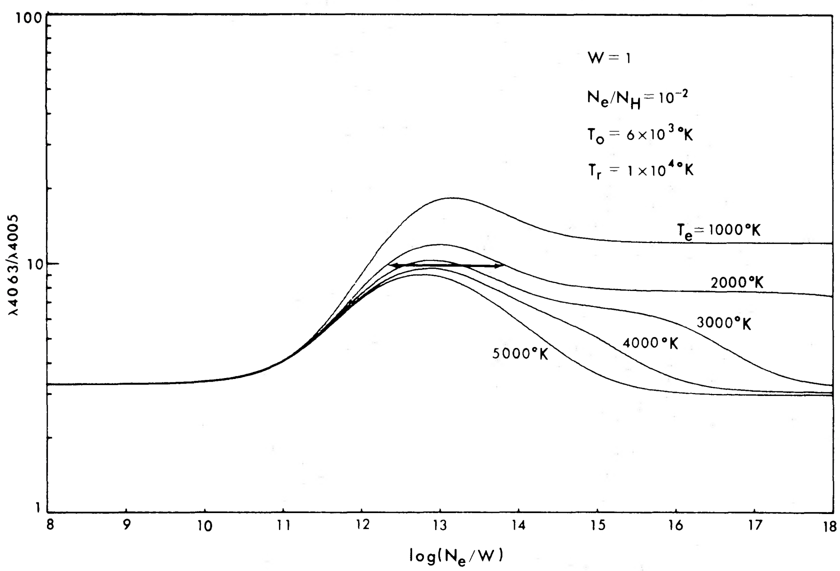

FIG. 4b

FIG. 4.—(*a*) and (*b*). The ratios λ4063/λ4143 and λ4063/λ4005 as a function of log (N_e/W) for different values of T_e. The observed line ratios are indicated by the arrows.

derivation and discussion of the equations used, see Willson (1972).

The intensity of the exciting λ3969 line may be characterized in another way: define

$$E = B_{\lambda 3969}(T_r)/B_{\lambda 3969}(T_0)\,, \qquad (6)$$

where $B_\lambda(T)$ is the Planck function at wavelength λ. E is the ratio of the intensity in the exciting line to the intensity of the underlying continuum, and so is directly related to the observed Ca II H or Hε intensity. For very low N_e and T_e, we expect the line ratios to depend only on the radiative parameters T_0 and T_r. In fact, they are determined by E alone for a wide range of T_0 and T_r.

To summarize, our model consists of a five- or 12-level Fe I atom, located in a gas of electron density N_e and temperature T_e. Impinging on our atom is a radiation field at temperature T_0 originating from a star which may be some distance away, and so diluted by a factor W. The radiation field has a spike of intensity equal to E times the continuum intensity at 3969 Å; this coincides with the transition 1–11 in the model atom. When radiative transitions dominate, level 11 is overpopulated due to pumping from level

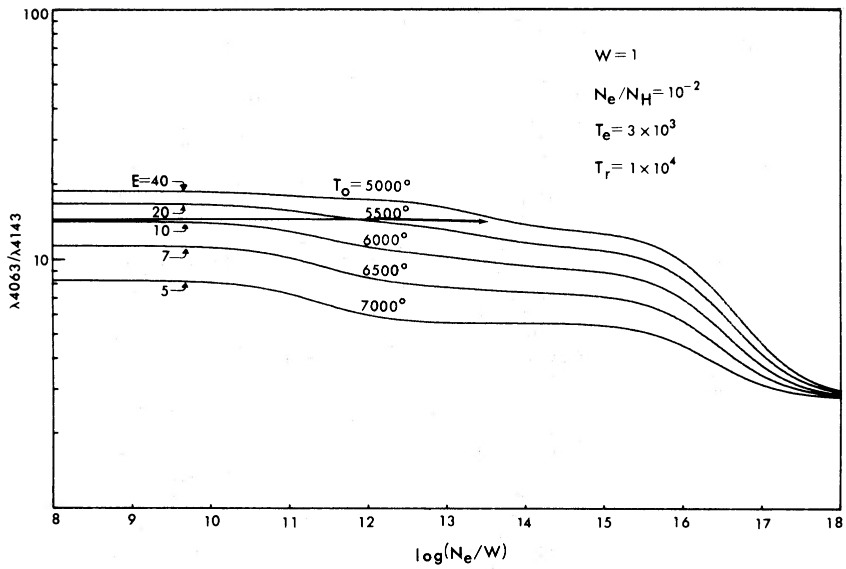

FIG. 5.—The ratio λ4063/λ4143 as a function of log (N_e/W) for varying T_0. Note that the upper limit on N_e/W is not very sensitive to changes in T_0. The arrow indicates the line ratio observed for RW Aur.

1. Photons in the lines λλ4063, 4132 emitted by transitions 11–3 and 11–2 are assumed not to be absorbed before escaping the system.

III. RESULTS OF THE STATISTICAL EQUILIBRIUM CALCULATIONS

The results of solving the statistical equilibrium equations for a variety of conditions are displayed in Figures 3–6. The ratio of intensities λ4063/λ4143 is shown as a function of N_e/W for various choices of T_0, T_r, T_e, and W, and λ4063/λ4005 is shown as a function of N_e/W for different values of T_e and W, with $N_p/N_H = N_e/N_H = 0.01$ used throughout.

Figures 3*a* and 3*b* show the line ratios λ4063/λ4143 and λ4063/λ4005 as a function of N_e/W for values of W ranging from 1 to 10^{-12}. It is apparent from figures 2 and 3 that for a wide range of W, N_e/W and N_e/N_H uniquely determine the line ratio λ4063/λ4143. The low-density behavior of λ4063/λ4005 is not purely a function of N_e/W only if $W < 10^{-6}$. The high-density drop of λ4063/λ4005 is given by N_e/W for W between 1 and 10^{-2}; for $W \leq 10^{-4}$ the dependence is more nearly on N_e. These features all represent a balance

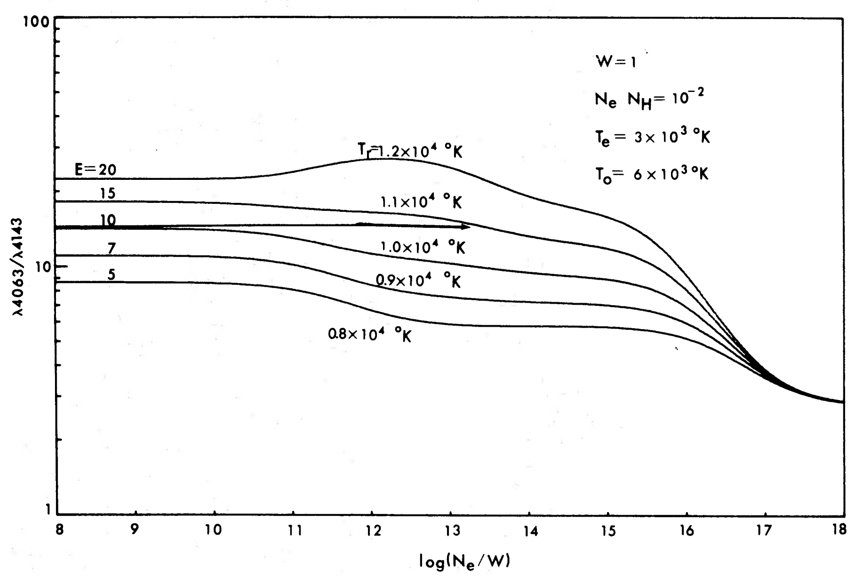

FIG. 6.—The ratio λ4063/λ4143 as a function of log (N_e/W) for varying T_r. Note that the upper limit on N_e/W is not very sensitive to changes in T_r. The line ratio observed in RW Aur is indicated by an arrow.

between collisional rates and radiative rates. For the rate equations, see e.g., equation (2) of Willson (1972), or Jefferies (1968, p. 125). The collisional rates are proportional to N_e (or N_H). Radiative excitation is always proportional to W. Radiative de-excitation is proportional to W when $(h\nu/kTW) \ll 1$; for fine-structure levels, this happens for $W \geq 10^{-2}$. For smaller W, radiative de-excitation is approximately independent of W, leading to the dependence on N_e noted above.

As was pointed out earlier, the line ratio $\lambda 4063/\lambda 4143$ represents the relative populations of the levels 11 and 10, while $\lambda 4063/\lambda 4005$ represents the relative populations of 11 and 12. The latter ratio is much less enhanced for low densities than is the former, indicating that level 12 is also highly overpopulated when level 11 is. For intermediate densities this ratio increases, then decreases again to its LTE value. To understand this we must consider the populations of all the levels at the lowest densities. For low densities and W close to 1, levels 2 and 3 may be over-populated by several orders of magnitude. The reason for this is the strong permitted transitions connecting 2 and 3 to the highly overpopulated level 11. Level 10, on the other hand, is populated mainly by transitions from level 2 and the depleted level 1. Thus levels 11 and 12 are overpopulated relative to level 10 at very low densities.

For intermediate densities, at these relatively low temperatures, collisions among the close levels 1, 2, and 3 dominate over radiative transitions between 1, 2, 3, and 10, 11, 12, thus keeping level 12 from being overpopulated. Thus as the density increases the ratio $\lambda 4063/\lambda 4005$ increases. The low-density behavior of $\lambda 4063/\lambda 4005$ thus represents a balance between radiative and collisional transition rates between fine-structure levels. Since collisions with neutral hydrogen atoms dominate the fine-structure transitions, the fact that $\lambda 4063$ is enhanced and $\lambda 4005$ is not gives us a lower limit on N_H which is of the form $N_H \geq f(T_0, T_r, T_e)W$ as long as $W \geq 10^{-6}$.

The behavior of the ratio $\lambda 4063/\lambda 4143$ as a function of density can be simply understood. For very low densities, collisional processes do not enter in at all, and the ratio is determined by the radiative rates alone. Hence the ratio is independent of the density. For very high densities, collisional processes dominate all transitions, giving LTE values for the line ratio. The LTE values depend only on the electron temperature T_e—thus for high densities the ratio is again independent of N_e.

At intermediate densities two types of curves occur. The first type has a simple drop from the low-density (extreme non-LTE, hereafter referred to as ENLTE) limit to the LTE value. This is seen for example in figure 3*a*. The second type first rises above the ENLTE limiting value, then drops to the LTE value (see fig. 4 or fig. 5). This second type of curve is readily understood if we consider in detail which processes dominate at each point along the curve. Starting from the lowest electron densities, we have first the ENLTE limit, where radiative processes dominate all transitions. Then we have an intermediate density range where collisions dominate transitions among the lower levels, numbered 1, 2, and 3 in the model (fig. 1). Collisions transfer atoms from levels 2 and 3 into the lowest level, level 1, which has been depleted by pumping to level 11. The transfer makes more atoms available for pumping which in turn enables the selective excitation to appear more strongly, and so the curve rises. Soon, however, collisions begin to dominate other transitions, and the curve turns down to the LTE limit for high densities.

In the discussion which follows, the term "cutoff value" refers to the narrow range of electron densities in which the line ratio drops from markedly enhanced to its LTE value.

In figure 4 we see the effect of varying T_e, for $T_0 = 6000°$ K and $T_r = 10{,}000°$ K. A number of such curves were calculated for different T_0, T_r pairs bracketing the conditions expected in T Tauri stars, where enhanced $\lambda\lambda 4063$, 4132 emission is observed. This particular T_0, T_r corresponds to an enhancement of the radiation field at $\lambda 3969$ of $E = 10$. We note that varying T_e primarily affects the value of N_e where the curve cuts off toward LTE, and that for low temperatures the dependence is quite strong. This is easily understood: T_e and N_e together determine the magnitude of the collisional excitation and de-excitation rates relative to the radiative rates, with the dependence roughly of the form $N_e \times \exp(-hc/\lambda k T_e)$ for a given N_H.

Figure 5 shows the effect of varying T_0, and figure 6 the effect of varying T_r. The enhancement E is indicated for each curve, and also the observed line ratios. $E \gtrsim 10$ is required for the calculated line ratio to be as large or larger than the observed one; $E \gtrsim 10$ corresponds to $T_r \geq 10^4$ ° K if $T_0 = 6000°$ K. For both of these we note that for a variation in T_0 or T_r of $\pm 1000°$ K the cutoff value of N_e is the same within an order of magnitude, as long as E is large enough. Further, T_0 may be estimated from the color of the star to well within 1000° K. T_r (or E) is also easily estimated from the intensity of the Ca II H-line and Hϵ. For higher T_0, T_r the errors introduced by uncertainties in T_0 or T_r are even smaller.

IV. IONIZATION LIMITS

Since $\lambda\lambda 4063$, 4132 are lines of neutral iron, a sufficient number of neutral iron atoms must be present if these lines are to be strong. The ionization equilibrium thus gives a further limit on the conditions allowing enhanced emission.

Low densities and high temperatures favor Fe II over Fe I. Therefore we do not expect to find strong $\lambda\lambda 4063$, 4132 emission from a gas with high temperature or low density. To translate this into quantitative limits requires information about the ionization equilibrium, and thus must be calculated by detailed consideration of the dominant mechanisms for ionization and recombination. It also requires knowledge of the volume of the emission region. Note that although a high degree of ionization may produce strong emission-line spectra by recombination, the mechanism for

TABLE 1

LINE INTENSITIES AND LINE RATIOS FROM GAHM 1970

Plate No. (Gahm)	Ca II H	Ca II K	Fe I λ4063	λ4143	λ4005	λ4063/λ4143	λ4063/λ4005
S1	149*	386*	56	4	6*	14	9
S2	overexposed	overexposed	48	3	5*	16	10
S3	47*	241*	38	2*	3*	19	13

* Intensities for these lines were underlined by Gahm, indicating that they were blended or that the continuum was ill defined.

producing the λλ4063, 4132 emission requires neutral atoms in the ground state. Further limits can be placed on the degree of ionization of iron from the observed limits on the strength of the recombination spectrum relative to the strength of the fluorescent lines. Again, quantitative limits require a more detailed model than we are considering here.

V. APPLICATION TO THE CIRCUMSTELLAR ENVELOPES OF T TAURI STARS

The lines λλ4063, 4132 are among the strongest emission lines in the spectra of many T Tauri stars (Joy 1945). Gahm (1970) has published a list of line intensities in emission and absorption for three plates of RW Aur. His intensities for λλ4063, 4143, and 4005 yield the line ratios given in table 1. Since factors not included in our analysis, such as absorption and re-emission and extra levels, can only diminish the line ratios, we conclude that the appropriate values for the ratios at the origin of the Fe I emission are

$$\lambda 4063/\lambda 4143 \geq 15\,, \quad \lambda 4063/\lambda 4005 \geq 10\,. \qquad (6)$$

Next, we must establish the values of the input parameters T_0, T_r, and T_e:

The parameter T_0, which describes the shape of the continuum emergy distribution, may be estimated in several ways. From the "average" spectral type for RW Aur, dG5e, we find $T_{\rm eff} \simeq 5500°$ K and $T_{\rm color} \simeq 6000°$ K for the visible portion of the spectrum. Herbig (1962) lists measurements of RW Aur yielding color temperatures between 4000 and 7000° K at different phases.

The *UBVRIJHKLM* colors of Mendoza (1968) for RW Aur can be fitted with $T_0 \simeq 5000$–$6000°$ K, the exact value depending on the corrections made for contributions to U, B, and V by emission lines. Kuhi (1969) estimates that emission lines may introduce errors of 10 percent or more in the continuum measurements. The underlying spectrum may also contain Fe I absorption lines—thus reducing the radiation field at the appropriate wavelengths and lowering T_0. These effects are difficult to estimate without a specific model; however one source of uncertainty for T_0 remains larger than these. T_0 probably varies with time. Without simultaneous measurements of the Fe I lines and the continuous energy distribution, the best we can do is a rough guess. $T_0 \simeq 6000°$ K for RW Aur near maximum is consistent with all the above measurements, and is used here.

The parameters T_r or E, giving the strength of the Ca II H exciting line, can be estimated in two ways. First, Gahm's listed intensities for Ca II H and Hε, about 50–150 in units of flux in 100 mÅ of the continuum, indicates an E of at least 10, and more if the observed width of the line, ~1 Å, is due to the overall velocity field of the outflowing gas (see Kuhi 1964). With $T_0 = 6000°$ K this gives $T_r \geq 10{,}000°$ K. There is a further check on T_r: if we assume a T_r which is too low, the calculated line ratios will lie *below* the observed ratios. In order to have the calculated value of λ4063/λ4143 *above* the observed values of 15–20 we must have $T_r > 10{,}000°$ K—see figure 6.

None of the conclusions about the circumstellar envelope of RW Aur that will be drawn from this analysis are very sensitive to T_0 and T_r. So estimates of $T_0 = 6000° \pm 500°$ K and $T_r > 10{,}000°$ K are probably sufficient. The electron temperature T_e at the source of the Fe I emission is more crucial to the upper limit on the density, and more difficult to estimate.

As we saw in § IV, an upper limit on T_e may be obtained from the requirement that enough neutral iron atoms be present. The question of the ionization equilibrium in the circumstellar envelopes of T Tauri stars is very complicated, and we will not attempt to answer it here. T Tauri stars often show an ultraviolet excess, whose origin and strength at the ionization edge of Fe I is not known. Further, there are indications that at least in some T Tauri stars and related objects, a substantial fraction of the hydrogen is ionized by some unknown process (see e.g., Osterbrock 1958; Milkey and Dyck 1973). We shall not consider here the complex problems posed by hypothetical radiation fields.

It is important to try to obtain a lower limit on the electron temperature, because for low temperatures the range of densities permitted becomes very large (see figs. 4*a* and *b*). Since we do not yet know which region is producing the fluorescent lines, we do not know T_e. In order to progress, we will assume a temperature which is reasonable, and proceed to calculate limits on N_e and $N_{\rm H}$. Then we will try to determine where in the nebula the lines originate. If we can determine the local electron temperature in that region by any independent means, we can improve our limits on the density.

Schwartz (1973) has measured the intensities of the forbidden lines in the nebula surrounding T Tauri. He finds for the outer portion of the nebula $7000°\ {\rm K} \leq T_e \leq 9000°$ K. That is too high for this to be the region producing the Fe I lines: first because the iron will be mostly ionized in this region; and second, because the fluorescent lines are not favored for $T_e \geq 5000°$ K (see figs. 4*a* and *b*).

Milkey and Dyck (1973) and Dyck and Milkey (1972) fit the continuous spectra of several hotter T Tauri–like stars with free-free emission for electron-ion encounters. They found $T_e \simeq 3000°$ K gave the best fit in the infrared for a wide range of stellar temperatures, with at least 10 percent of the hydrogen ionized. The *UBVRIJHKLM* colors of Mendoza (1968) for RW Aur may be fitted in the same way. Assuming free-free emission in a large shell to account for at least part of the infrared excess yields $T_e \simeq 3000°$ K. However this assumption is questionable for the cooler T Tauri stars. Schwartz's measurements of Hα and Hβ fluxes in T Tau gave an emission measure $N_e^2 V = 2 \times 10^{56}$ cm^{-3}, in agreement with the density and size of the ionized circumstellar envelope Kuhi used to fit the emission line profiles. Using equation (10) of Dyck and Milkey (1972), we can estimate the emission measure from Mendoza's (1968) infrared measurements for RW Aur and from Schwartz's (1973) measurements for T Tau. If free-free emission at $T_e \simeq 8000°$ K is to account for the infrared excess of these atoms, $N_e^2 V > 10^{58}$ cm^{-3} is required. This is much larger than was found from the hydrogen lines. Thus most of the infrared excess in these cooler stars is probably produced by dust with $T \lesssim 3000°$ K.

Since the neutral iron producing the fluorescent lines probably resides in a cool part of the nebula, we will estimate T_e to be $\simeq 3000°$ K. After we have established where the Fe I lines are formed, we can improve this estimate and our limits on N_e and $N_{\rm H}$.

From the calculations for the two line ratios for RW Aur, using $T_e = 3000°$ K, we find $N_e/W \lesssim 10^{16}$ if hydrogen is more than 10 percent ionized and $N_{\rm H}/W \lesssim 10^{16}$ if hydrogen is less than 10 percent ionized—see figures 2 and 3. We also find $N_{\rm H}/W \geq 10^{14}$ if $W \geq 10^{-6}$, for all values of $N_e/N_{\rm H}$ tested. To translate these into limits on N_e or $N_{\rm H}$ we must know W, i.e., we must determine whether there is appreciable dilution of the radiation field. This is equivalent to determining where in the circumstellar shell the Fe I lines originate. The possibilities are summarized in table 2, for a spherically symmetric envelope.

The expected $N_{\rm H}$ and N_e and the velocities in table 2 are obtained as follows: the photospheric densities are typical values for a G5 dwarf from Allen (1963). The last, interstellar, values are typical values for a dense interstellar cloud taken from Heiles (1971). The intermediate densities and the velocities are obtained using Kuhi's (1966) values for the velocity and the density at the inner edge of the emission-line region (the chromosphere) for RW Aur and letting them drop according to Kuhi's (1964) equations (1) and (2). We also note that $N_e \leq 10^{13}$ in the chromosphere if we use Gahm's (1970) list of hydrogen lines presumed present. The electron densities are obtained from the hydrogen densities by assuming that at the surface, the hydrogen is neutral and the metals ionized, so $N_e \simeq 10^{-4} N_{\rm H}$; in the chromosphere, H is ionized almost completely—$N_e \simeq N_{\rm H}$ to $N_e \simeq 0.1 N_{\rm H}$; in the "observable nebula" $N_e/N_{\rm H} \lesssim 0.1$.

The limits on the hydrogen density and the electron density are seen to be consistent with the expected densities in the photosphere and in the circumstellar envelope obtained from Kuhi's (1964, 1966) fitting of the emission line profiles. Thus the density limits give us no clue as to where in the system the Fe I lines originate. This is unfortunate, since it prevents us from estimating the electron temperature directly from the distances and densities. We must find some other way of determining where in the system the Fe I lines are formed, in order to check T_e and interpret our results.

Walker (1972) lists some radial velocities of emission and absorption components of several lines including some hydrogen lines, Ca II K, and Fe I λ4063

TABLE 2

Dilution Factors and Densities as a Function of Distance from the Star

R/R$_*$	W	$N_{\rm H}$ from Fe I (cm^3)	Expected $N_{\rm H}$* (cm^3)	Expected N_e* (cm^3)	N_e from Fe I (cm^3)	V (km s^{-1})	Region
1.......	0.5	10^{13}–10^{16}	$\sim 10^{17}$	$\sim 10^{13}$	$\leq 10^{16}$	0? 425?	photosphere
10.......	2×10^{-3}	10^{10}–10^{13}	$\sim 10^{10}$	10^{9}–10^{10}	$\leq 10^{13}$	45	chromosphere or H II region
10^2......	2×10^{-5}	10^{8}–10^{11}	$\sim 3 \times 10^{8}$	$\leq 10^{7}$	$\leq 10^{11}$	15	Fe I lines?
10^4......	2×10^{-9}	$\leq 10^{7}$	$\sim 3 \times 10^{5}$	$\leq 10^{3}$	$\leq 10^{7}$	1.5	
10^6......	2×10^{-13}	$\leq 10^{3}$	$\sim 3 \times 10^{2}$, (10^4†)	$\leq 10^{-1}$ (10^3†)	$\leq 10^{3}$	0.15	directly observable region
10^7......	2×10^{-15}	$\leq 10^{1}$	$\lesssim 10^{3}$	$\leq 10^{-1}$	$\leq 10^{1}$	...	interstellar medium

* Expected values for $N_{\rm H}$ and N_e are obtained from Kuhi's (1964, 1966) model combined with photospheric and interstellar values, as described in the § V.

† Comparison value from Osterbrock's (1958) study of the nebula surrounding T Tauri; Schwartz (1973) finds $N_{\rm H} \simeq N_e \simeq 3 \times 10^3$–$10^4$ and $T_e \simeq 8000°$ K for that same nebula.

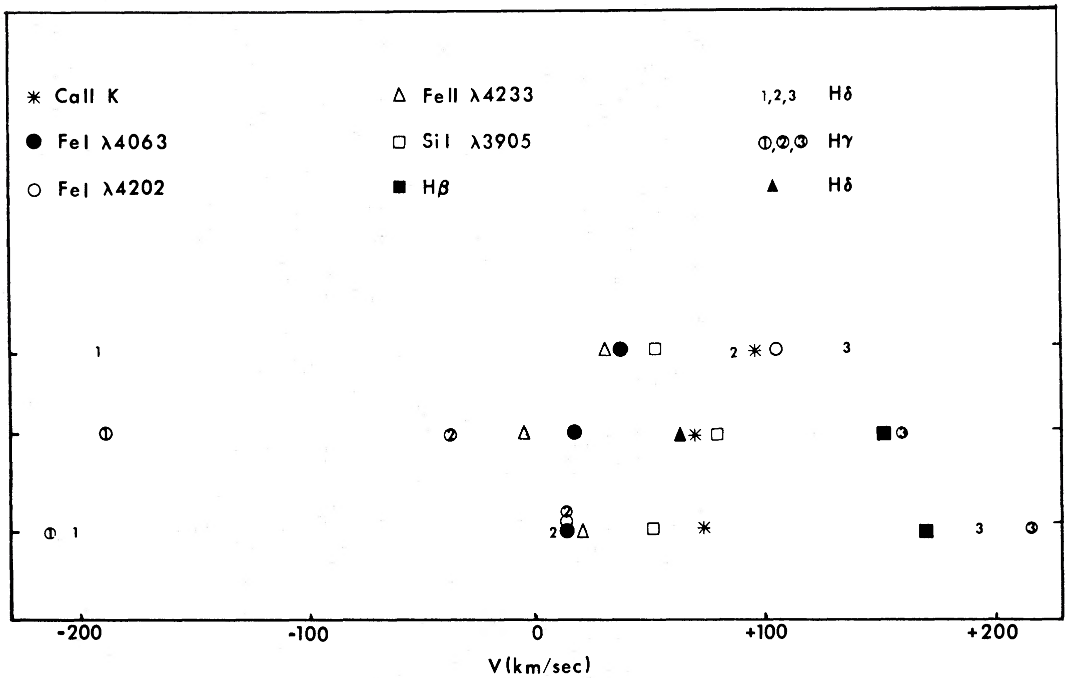

FIG. 7.—Velocity of emission lines and absorption components for HS Ori, from three plates by Walker 1972

for three plates of HS Orionis, a star similar to RW Aur and with strong Fe I λ4063 emission. The radial velocity of the Fe I line λ4063 is about that expected for the star on two plates and shows a small amount of redshift on a third. The Ca II K-line at λ3933 indicates material sinking with a velocity of 50–60 km s^{-1} relative to the Fe I lines on all three plates. No other pair of lines listed shows a constant velocity difference. 50–60 km s^{-1} is almost exactly the velocity shift needed to superpose Ca II H (λ3968.470) and Fe I λ3969.261. This suggests that what determines where the Fe I lines will be formed is the velocity field, not the density; that the exciting photons travel through the nebula until their wavelength, shifted due to their origin in a rapidly moving region, matches that of the Fe I transition in the surrounding gas. If a large velocity shift is required for the Fe I emission lines to be formed then we expect a correlation between high-velocity envelopes and Fe I λ4063 intensities. T Tauri, RW Aur, and five other stars are listed in table 3, with velocity differences, Ca II and H I line intensities, and fluorescent line intensities taken from Joy (1945). The Fe I lines decrease uniformly in intensity as the velocity difference decreases, while the intensity of the Ca II and H I lines show no such correlation. This is further qualitative support for this model. Also Kuhi's (1964, 1966) correlation between mass-loss rate and emission-line intensity class is exactly what one would expect if the ejection velocity determines the strength of the fluorescent lines.

The fluorescent iron lines may be excited by Ca II H emission which has been redshifted, or by Hϵ emission which has been blueshifted, as seen by the fluorescing iron atom. The observed velocity shift of 60 km s^{-1} in HS Ori tells us nothing about which of these possibilities is likely to be true, since a velocity shift of the

TABLE 3

RADIAL VELOCITIES AND LINE INTENSITIES FOR SEVEN T TAURI STARS FROM JOY 1945

Star	ΔV(abs. − em.)	Fe I λ4063	Fe I λ4143	Ca II H	Ca II K	Hϵ*	Hβ
UZ Tau......	no absorption line spectrum	8	1	25	50	2	30
S CrA	no absorption line spectrum	5	2	20	15	...	30
RW Aur	+84	5	1	35	45	...	40
XZ Tau......	+67	4	1	25	25	...	40
UY Aur	+33	3	...	50	45	4	40
T Tau	+5	2	0	35	40	2	40
R Mon	−9	...	...	1	3	...	15

* Hϵ intensities quoted by Joy (1945) are uniformly much lower than that expected from the other Balmer lines. This may be due to the blending of Hϵ with Ca II H, or possibly the absorption of Hϵ by the Fe I.

same magnitude is required in either case. For stars which are losing mass, there are four configurations allowed by the hypothesis that the Fe I lines are produced in a region where the exciting line has been shifted to $\lambda \simeq 3969.27$ Å:

1) The emission lines are produced in a rapidly rising region near the star; Fe I emission comes from a region farther out, which is moving more slowly. The iron atom absorbs blueshifted Hϵ emission; we observe Fe I lines at approximately the same velocity as the star, and Hϵ and the other primary emission lines are blueshifted. This is the model assumed in table 2.

2) Fe I lines are formed in an essentially motionless region in or near the photosphere; the primary emission lines are produced in a rapidly expanding envelope above this region. In this case the iron atom is excited by redshifted Ca II emission, but an external observer sees the Ca II and H emission lines blueshifted with respect to the Fe I lines and the stellar absorption spectrum.

3) Fe I lines form in a rapidly rising region near the star, excited by Hϵ emitted from a slower region farther out.

4) Ca II emission from a slowly moving region near the star excites Fe I fluorescence in a more rapidly rising region farther from the star.

For cases 3 and 4, an external observer sees the primary emission lines of H and Ca II redshifted with respect to the Fe I lines, but both the Ca II lines and the Fe I lines will be blueshifted with respect to the underlying stellar absorption-line spectrum. In HS Ori, Ca II K was redshifted with respect to Fe I, but also with respect to the expected velocity of the star; hence HS Ori must be accreting matter rather than losing it. For the present we will consider only stars such as RW Aur for which outflow of matter is indicated. Cases 3 and 4 require the fluorescent lines to be produced in a region which is moving *more* rapidly than the region producing the primary emission lines—but that region is already known to be moving rapidly with respect to the star. This seems unlikely; furthermore, this gives no explanation for the correlation between larger velocities for the emission-line region and more intense $\lambda\lambda$4063, 4132 shown in table 3. We therefore eliminate case 3 and case 4.

This leaves us with a choice of the first two possibilities. Case 2 has the fluorescent lines produced in or near the photosphere, beneath the envelope producing the other emission lines. This is unlikely for three reasons: first, iron is probably ionized in the photosphere. Since these stars generally have a large ultraviolet excess, and since the hot, ionized emission-line region is close to the star, it seems likely that there are sufficient ultraviolet photons present to keep the iron ionized throughout the region between the photosphere and chromosphere. Second, for many of these stars, particularly those like UZ Tau and S CrA that have the brightest $\lambda\lambda$4063, 4132 emission, the photospheric absorption-line spectrum is not seen. This may be because the overlying chromosphere and circumstellar envelope is optically thick, or because emission from the chromosphere and the circumstellar envelope dominates at the wavelengths of the lines. It is difficult to see how the fluorescent Fe I lines could be as strong as they are for these stars if they were formed below the envelope. (These objections also apply to case 3.) The third objection to case 2 is that it implies that the envelope is being accelerated. An accelerated envelope produces flat-topped emission lines, unlike those found in most T Tauri stars (see Chandrasekhar 1934; Kuhi 1964). (This objection also applies to case 4.)

A similar analysis may be made for stars such as HS Ori which are still accreting matter. In this case, only two models are consistent with the observed difference in the radial velocities and with the presence of the fluorescent iron lines:

1) Ca II emission coming from a region with high infall velocity near the star excites Fe I emission in a slowly moving or stationary region farther out.

2) Hϵ emission from the rapidly moving chromosphere near the star excites Fe I from a stationary region below the chromosphere.

The second case here is improbable, since it requires the infalling matter to decelerate and cool simultaneously. Thus the acceptable model for the stars with accretion is quite similar to the most probable model for the stars showing mass loss: a high-velocity chromosphere near the star, producing Hϵ and Ca II H emission, and fluorescent lines of iron produced farther from the star, in a more slowly moving region. The fact that both RW Aur and HS Ori show fluorescent lines is therefore a consequence of the double coincidence of Fe I λ3969 with Ca II H and Hϵ.

Thus the Fe I lines are probably formed outside of the chromospheric region, beyond 10 or 100 stellar radii, where iron is mostly neutral and where the gas has slowed to 55 or 60 km s^{-1} slower than the expansion velocity at the chromosphere. This may explain also why for example T Tau shows weaker Fe I fluorescent lines than RW Aur, even though its Ca II lines are nearly as strong (see e.g., Joy 1945 for rough line-intensity estimates for T Tau and RW Aur). Kuhi (1964) mentions that while in most of the T Tauri stars whose profile he fitted deceleration of the envelope was required, the profiles for T Tau were ambiguous. He suggested that as stars approach the main sequence the mass loss slows down and a solar-wind–type acceleration process becomes more important, and that for T Tau this may be happening. This is also consistent with the average difference between the velocities of the emission- and absorption-line spectra for RW Aur and T Tau listed by Joy (1945): for RW Aur it is 84 km s^{-1}, for T Tau it is only 5 km s^{-1}.

In case 1 the fluorescent lines are excited by Hϵ, not the stronger Ca II H-line. We must next check whether Hϵ is strong enough to produce the observed Fe I emission for RW Aur. Gahm does not list an intensity for Hϵ, since in the spectrum we see it is blended with Ca II H. However, we can estimate what its original intensity must have been from the strength of the other Balmer lines. Interpolating between the intensities for

Hβ, Hγ, Hδ, H8, and H11 that Gahm lists, using the known transition strengths for the Balmer lines, leads to an estimated Hϵ intensity of about 30 in units of the intensity in 100 mÅ of the continuum. If the Fe I sees an Hϵ profile that has a width $\leqslant 30$ km s^{-1}, then the central intensity will be adequate to produce the observed ratio λ4063/λ4143. It is reasonable to assume the profile of Hϵ seen by the iron atom is no broader than this.

Joy (1960) stated that the strength of Ca II K in T Tauri stars is usually nearly equal to that of Hγ. Since the intensity ratio Ca II K/Ca II H for an optically thin envelope is 2, and Hγ/Hϵ is also about 2, this indicates that for most T Tauri stars at the origin of the emission lines the intensities of Hϵ and Ca II H should be nearly equal. Thus it is not unreasonable to suspect that Hϵ and not Ca II H excites the fluorescent iron lines.

It is also interesting to note, in support of Hϵ as the exciting line, that all the fluorescent processes listed in Gahm's table 2 have exciting lines with longer unshifted wavelengths than the fluorescent lines *except* Ca II H (λ3968.47) and Fe I λ3969.27. If Hϵ (λ3970.07) is instead responsible for λλ4063, 4132 then there are no exceptions to this rule, and the same geometry will produce all the fluorescent lines Gahm found for RW Aur.

We conclude that the Fe I lines are probably formed at more than 10 stellar radii from the star, in the circumstellar envelope. Since the Fe I fluorescent lines are characteristic of T Tauri stars, all T Tauri stars must have extended envelopes. The fact that forbidden lines of e.g., [S II] are also characteristic of T Tauri stars supports this conclusion. For some T Tauri stars, envelopes 10^5–10^6 stellar radii in extent have been observed; an envelope of 10^4 stellar radii or less is too small to observe directly. The presence of strong Fe I λλ4063, 4132 emission probably also indicates a high rate of mass loss, with matter ejected from the surface of the star and then decelerating as it moves away, although λλ4063, 4132 emission may also be present in some stars which are accreting matter.

VI. SUMMARY

We conclude that the selective excitation of Fe I $y\,^3F_3^o$ by Ca II H can reproduce the observed line intensities for T Tauri stars. Whenever λλ4063, 4132 are observed to be enhanced, an upper limit of N_e or $N_{\rm H}$ is implied. The limit is of the form

$$N_e \leq W \times f_1(T_e, T_0, T_r)\,, \quad N_e/N_{\rm H} \geq 0.01\,, \qquad (7)$$
$$N_{\rm H} \leq W \times f_2(T_e, T_0, T_r)\,, \quad N_e/N_{\rm H} < 0.01\,,$$

for almost all values of N_e, W, T_e, T_0, and T_r. The value of the functions f_1 and f_2 for a given situation may be found from the graphs of line ratio versus N_e/W. For cases with $\tau \geq 1$, this upper limit will be less than that calculated for $\tau \ll 1$, since some of the photons in the enhanced lines will be lost to collisions in transit. The dependence of these functions on T_0 and T_r is generally weak. For RW Aur with $T_e = 3000°$ K we find

$$N_e \leq W \times 10^{16} \qquad (8)$$

or

$$N_{\rm H} \leq W \times 10^{16}\,.$$

An upper limit on T_e may also be obtained from the presence of these lines by adding one further condition: that the number of neutral iron atoms present must be sufficient to produce the observed intensity in the Fe I lines.

For RW Aur the densities allowed by the strength of the fluorescent lines are consistent with the densities expected in the photosphere or anywhere in the circumstellar envelope. Consideration of the velocity field in the envelope and observed radial velocities for the various lines in several stars led us to conclude that the fluorescent iron lines probably are excited by Hϵ and originate in that part of the envelope where velocity of expansion is 55 km s^{-1} less than that of the chromosphere. However, we cannot exclude the alternate possibility that the Fe I lines are formed far enough from the star (≥ 100 stellar radii) that the iron sees only a broadened blend of Ca II H and Hϵ. Strong fluorescent iron lines at λλ4063, 4143 in stars with emission lines blueshifted with respect to the underlying absorption spectrum are thus indications of violent mass-loss phenomena, with ejection of matter from the star at high temperature and velocity, and with the ejected matter cooling and decelerating as it gets farther from the star.

I would like to thank C. R. Cowley for suggesting this project, and for his help throughout. I am also grateful to G. H. Herbig for his suggestions. Appreciation is also due K. Everson, S. Willson, and numerous members of the Astronomy Department at the University of Michigan for criticisms and comments. This work was supported in part by the National Science Foundation.

REFERENCES

Allen, C. W. 1963, *Astrophysical Quantities* (London: Athlone Press).
Bahcall, J. N., and Wolf, R. A. 1968. *Ap. J.*, **152**, 701.
Breig, E. L., and Lin, C. C. 1966, *Phys. Rev.*, **151**, 67.
Chandrasekhar, S. 1934, *M.N.R.A.S.*, **94**, 534.
Dyck, H. M., and Milkey, R. W. 1972, *Pub. A.S.P.*, **84**, 597.
Gahm, G. F. 1970, *Ap. J.*, **160**, 1117.
Heiles, C. 1971, *Ann. Rev. Astr. and Ap.*, **9**, 293.
Herbig, G. H. 1945, *Pub. A.S.P.*, **57**, 166.
———. 1962, *Adv. Astr. and Ap.*, **1**, 47.
Jefferies, J. T. 1968, *Spectral Line Formation* (London: Blaisdell).
Joy, A. H. 1945, *Ap. J.*, **102**, 168.
———. 1960, in *Stellar Atmospheres*, ed. J. L. Greenstein (Chicago: University of Chicago Press), p. 653.
Kuhi, L. V. 1964, *Ap. J.*, **140**, 1409.

Kuhi, L. V. 1966, *Ap. J.* (*Letters*), **143**, 991.
———. 1969, 16eme Colloq. Int. d'Ap., Liège, p. 295.
Mendoza, E. E. 1968, *Ap. J.*, **151**, 977.
Milkey, R. W., and Dyck, H. M., 1973, *Ap. J.*, **181**, 833.
Osterbrock, D. E. 1958, *Pub. A.S.P.*, **70**, 399.
Schwartz, R. D. 1973, thesis, University of Washington, Seattle.
Walker, M. F. 1972, *Ap. J.*, **175**, 89.
Willson, L. A. 1972, *Astr. and Ap.*, **17**, 354.

L. A. WILLSON
A317 Physics, Iowa State University, Ames, Iowa 50010